Study of phase transitions in cathode materials for sodium-ion batteries

N.Yu. Samoylova, S.V. Sumnikov, O. Yu. Ponomareva, R.N. Vasin, M.E. Donets, E.A. Korneeva

Joint Institute for Nuclear Research, Dubna, Russia
rny03@nf.jinr.ru - N.Samoylova

I.A. Bobrikov

Centre for Cooperative Research on Alternative Energies (CIC energiGUNE), Basque Research and Technology Alliance (BRTA), Alava Technology Park, Albert Einstein 48, Vitoria-Gasteiz 01510, Spain

The Prussian blue systems

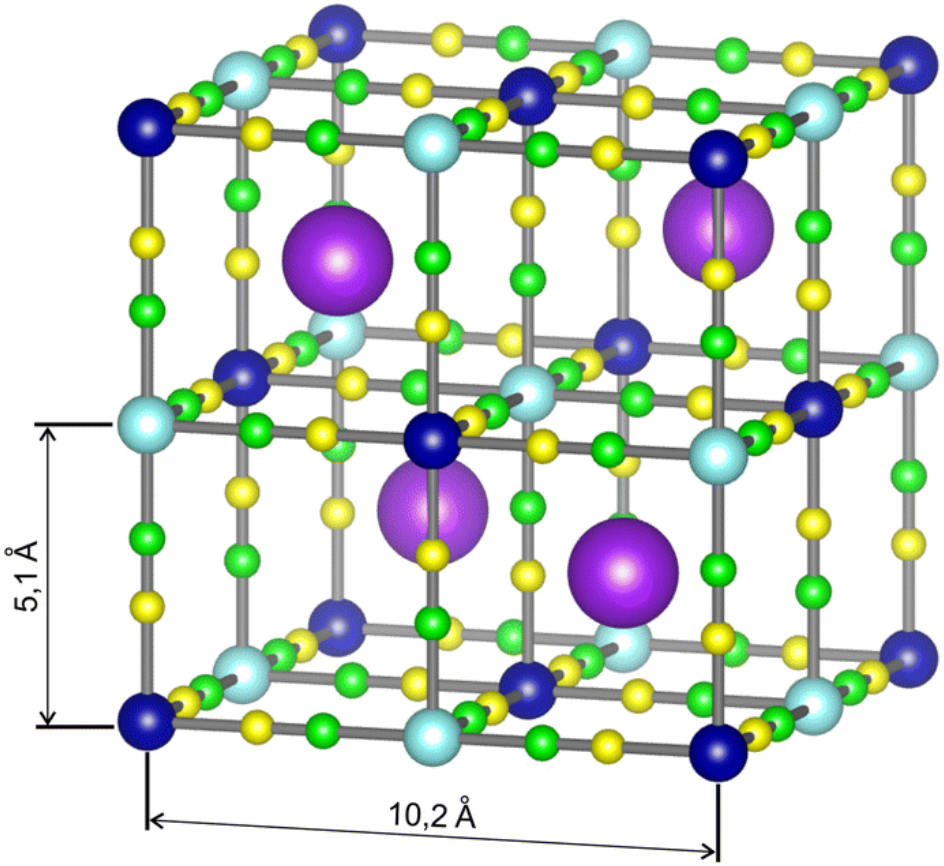

iron-II

iron-III

carbon

nitrogen

A^+ (e.g. Li^+, Na^+, K^+, NH_4^+)

Structure of Prussian blue according to the Keggin and Miles, 1936

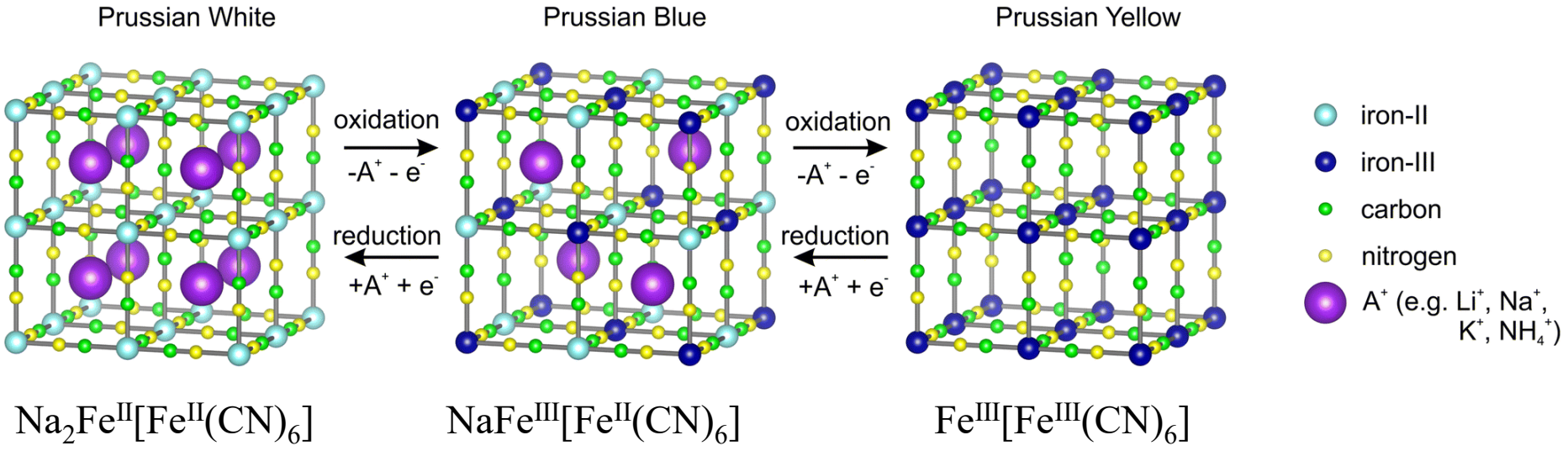

$Na_2Fe^{II}[Fe^{II}(CN)_6]$ $NaFe^{III}[Fe^{II}(CN)_6]$ $Fe^{III}[Fe^{III}(CN)_6]$

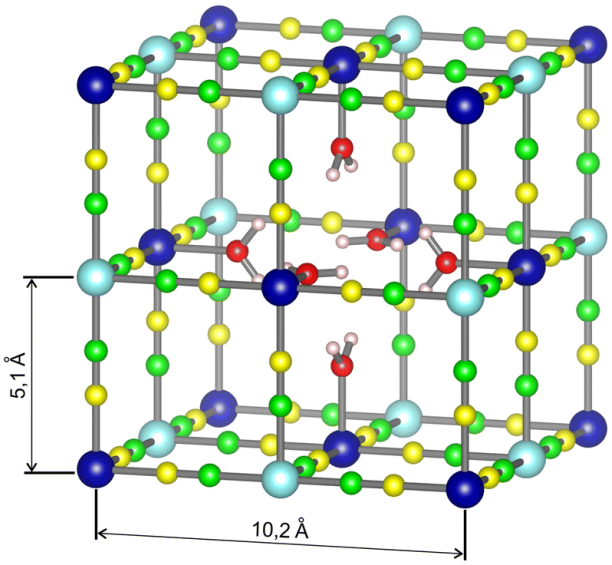

$Na_2Fe[Fe(CN)_6]_{1-y}\cdot\square_y\cdot mH_2O$

□ - $Fe(CN)_6$ vacancies,
y - their number

The origin aim is to study:

- the structural evolution of the PW material under dehydration during heating;
- the effect of the electrode annealing temperature on the PW structure and structural phase transitions during sodiation/desodiation (discharge/charge) processes, as well as the electrochemical properties of the material;
- the structural aspects of capacity loss during long cycling.

Material

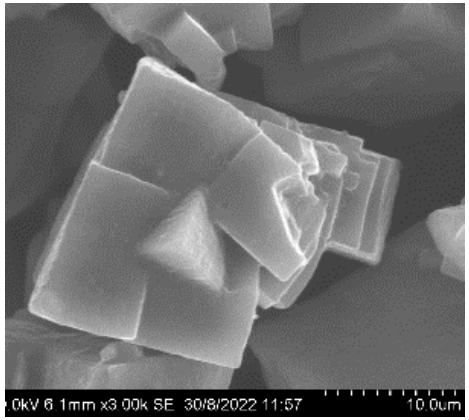

Commercial Prussian White, Fennac
(Altris, Uppsala)

XRD electrochemical cell

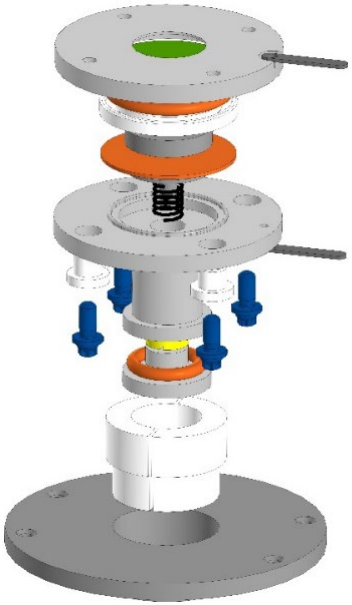

Operando X-ray diffraction measurements

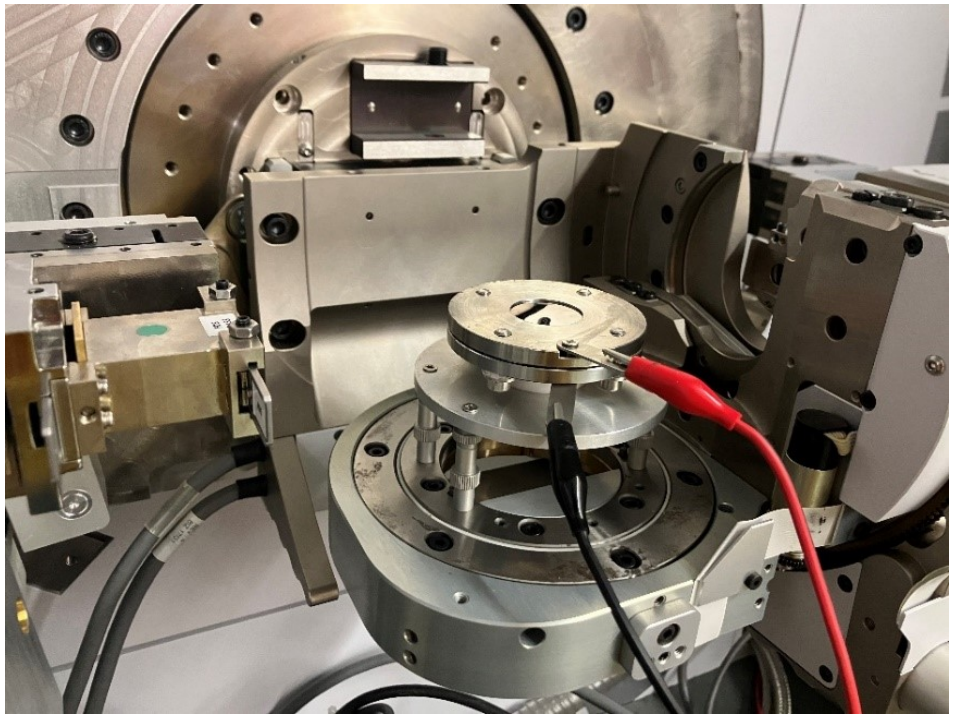

XRD experiment at Empyrean PANalytical diffractometer

Crystal structure of Prussian White

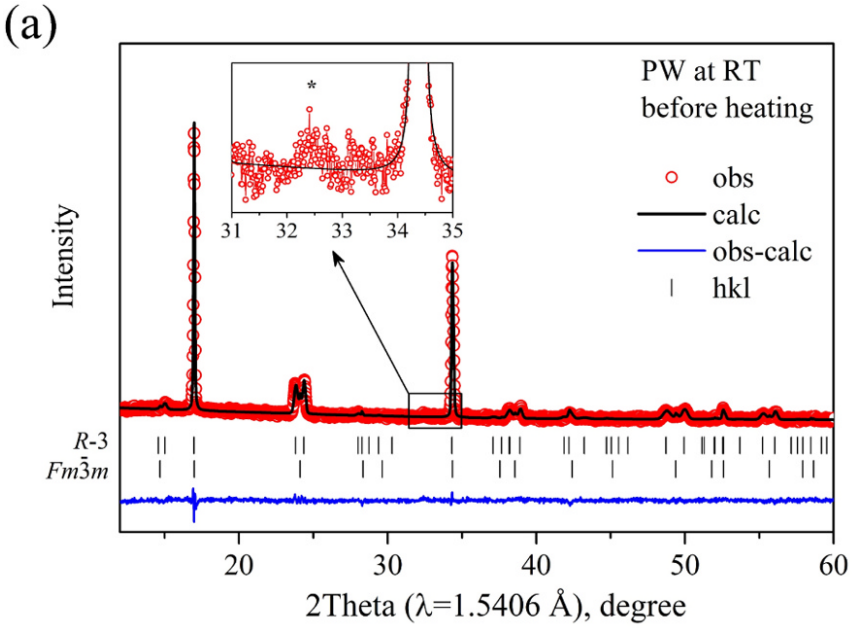

X-ray diffraction pattern of the PW powder at room temperature fitted with *F*m-3m and *R*-3 structures

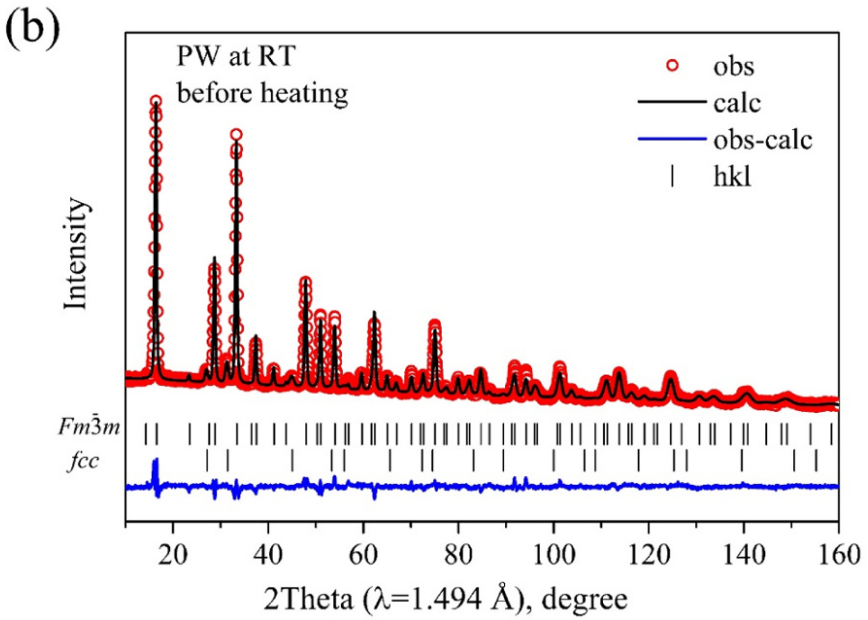

Neutron diffraction pattern of the PW powder at room temperature fitted with *F*m-3m structure

Phase transitions in the PW material during dehydration

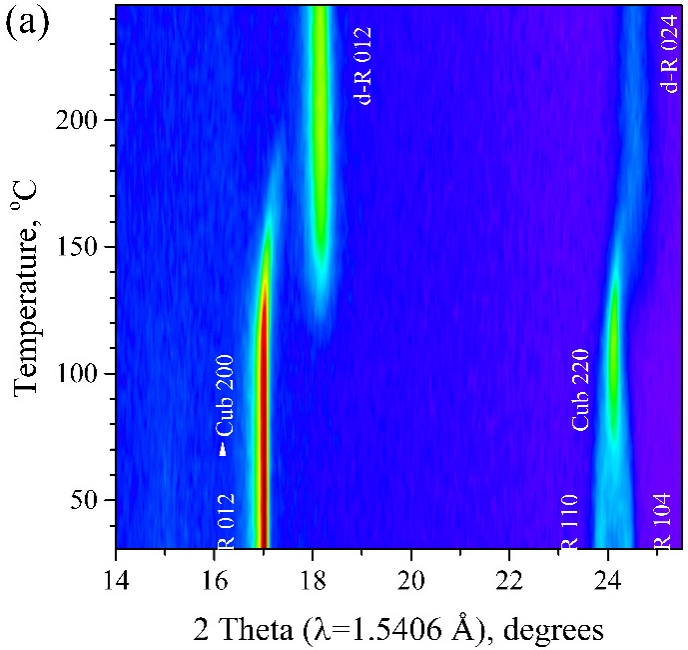

hydrated **rhombohedral** (R)
(sp. gr. *R*-3, *a* = 7.4682 Å, *c* = 17.683 Å) →

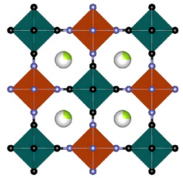

cubic (Cub)
(sp. gr. *Fm*-3*m*, *a* = 10.4322 Å) →

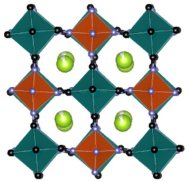

dehydrated rhombohedral (d-R)
(sp.gr. *R-3*, *a* = 6.5395 Å , *c* = 18.933 Å)

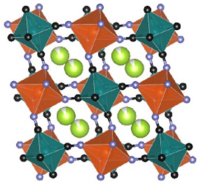

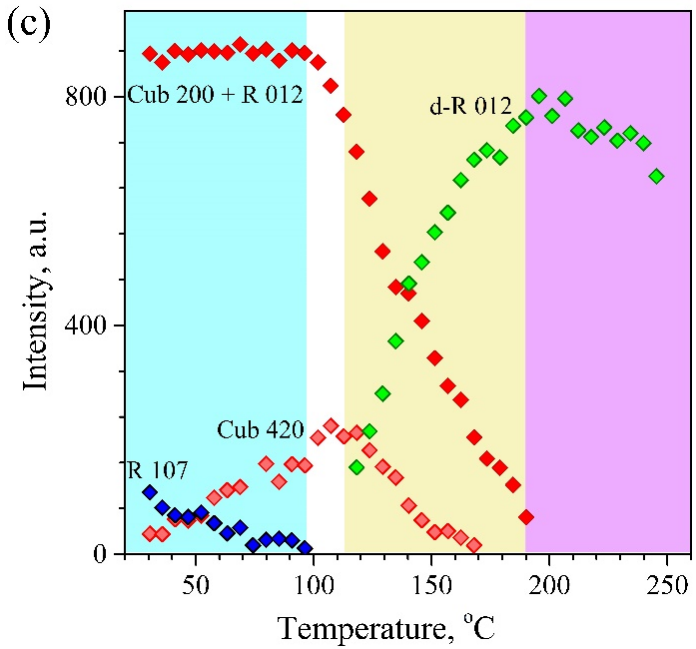

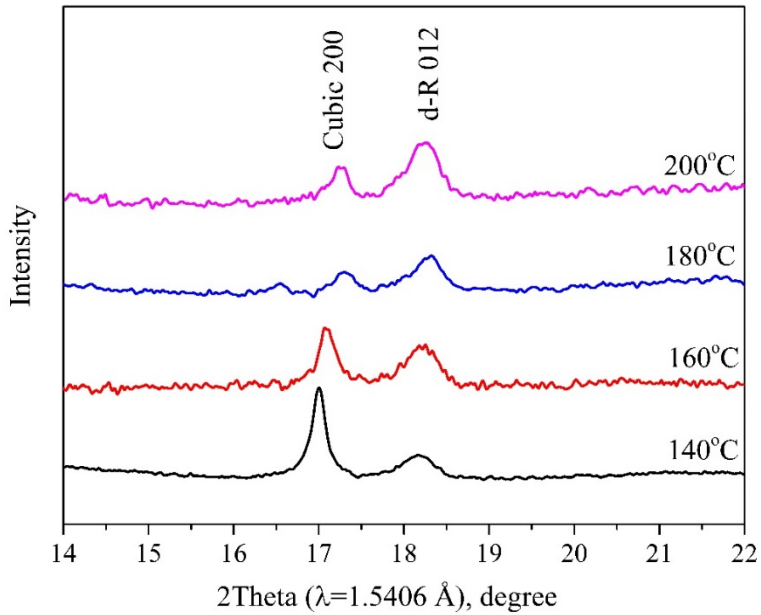

N.Yu. Samoylova et al., Peculiarities of charge-discharge processes in Prussian white electrodes with different level of dehydration, J. Alloys Compd. 983 (2024) 173849.

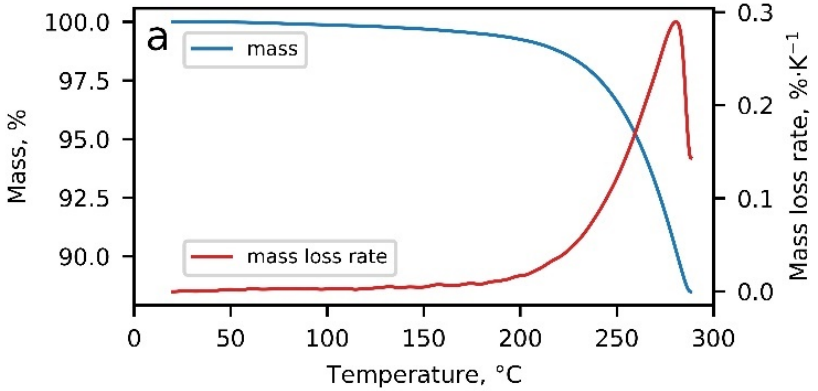

TGA curve

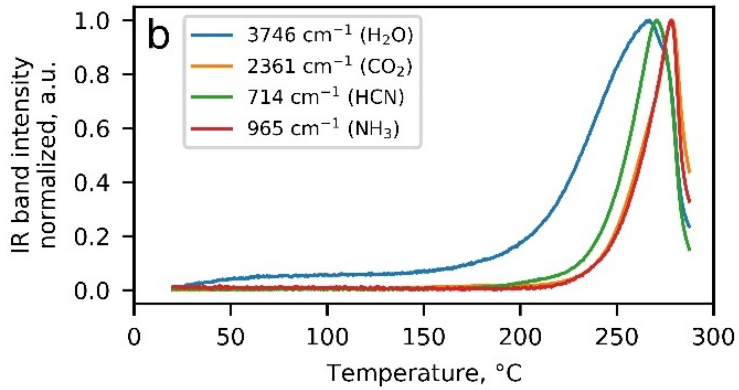

kinetics of gas evaporation under heating of the PW powder in N_2 atmosphere

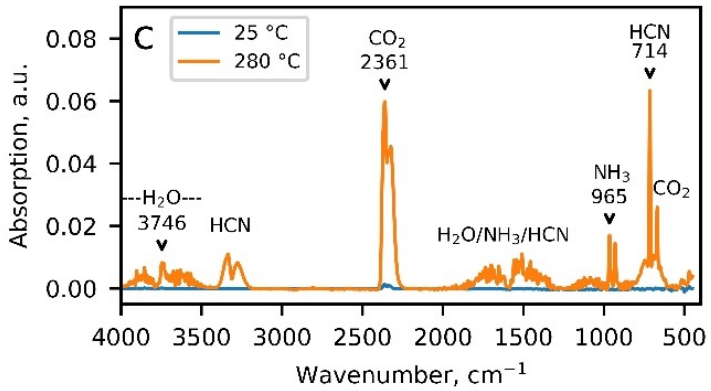

FTIR spectra of the gaseous PW decomposition products

N.Yu. Samoylova et al., Peculiarities of charge-discharge processes in Prussian white electrodes with different level of dehydration, J. Alloys Compd. 983 (2024) 173849.

1C = 170 mAhg^{-1}

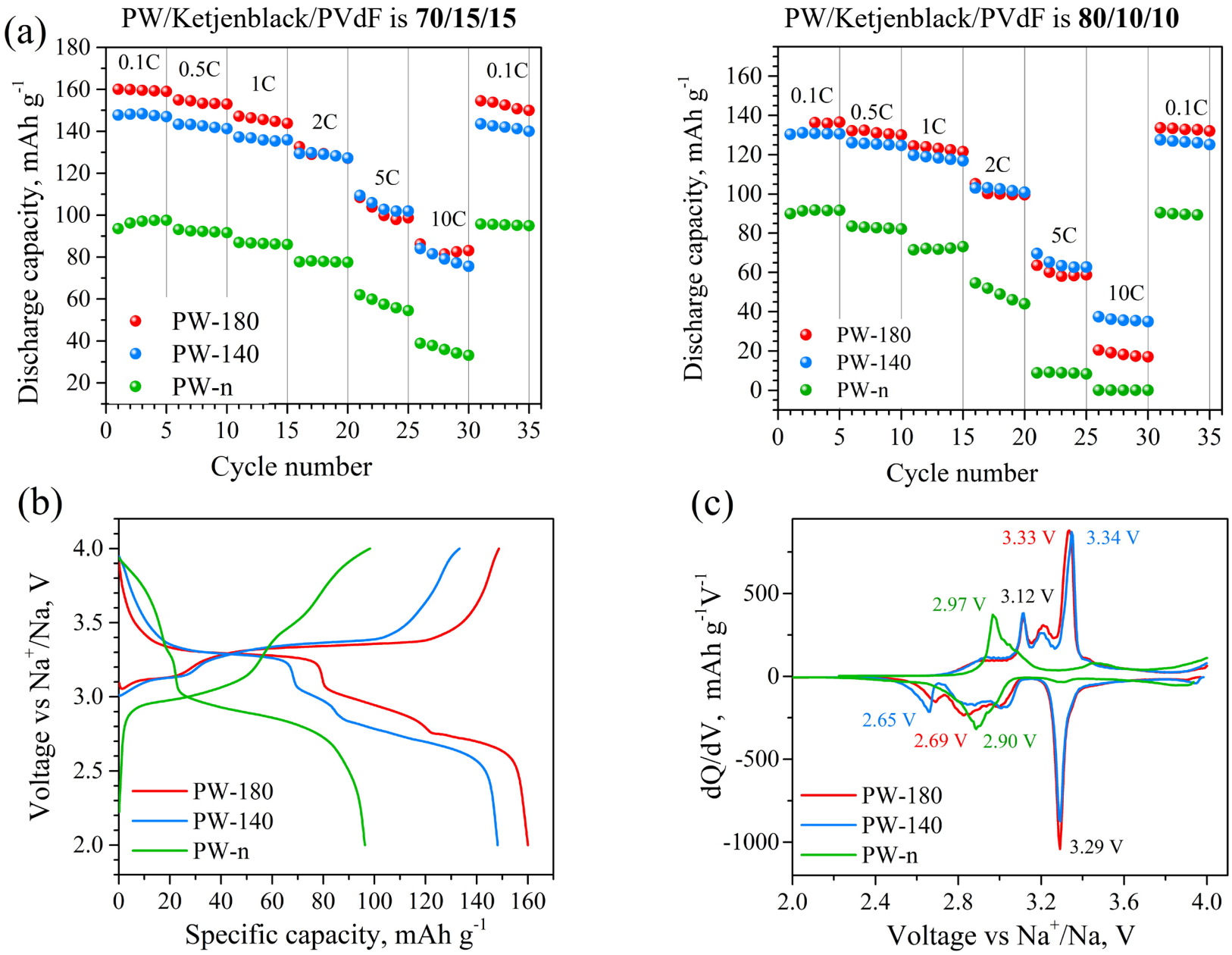

N.Yu. Samoylova et al., Peculiarities of charge-discharge processes in Prussian white electrodes with different level of dehydration, J. Alloys Compd. 983 (2024) 173849.

Madder et al. J. Mater. Chem. A, 2023, 11, 15778: PW/carbon add/CMC is **93.5/3/3.5**, 1C = 140 $mAhg^{-1}$

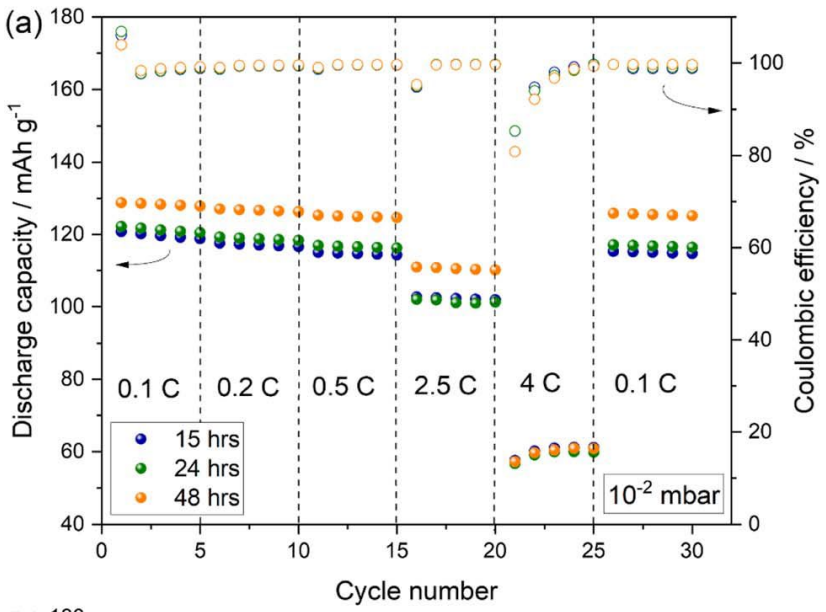

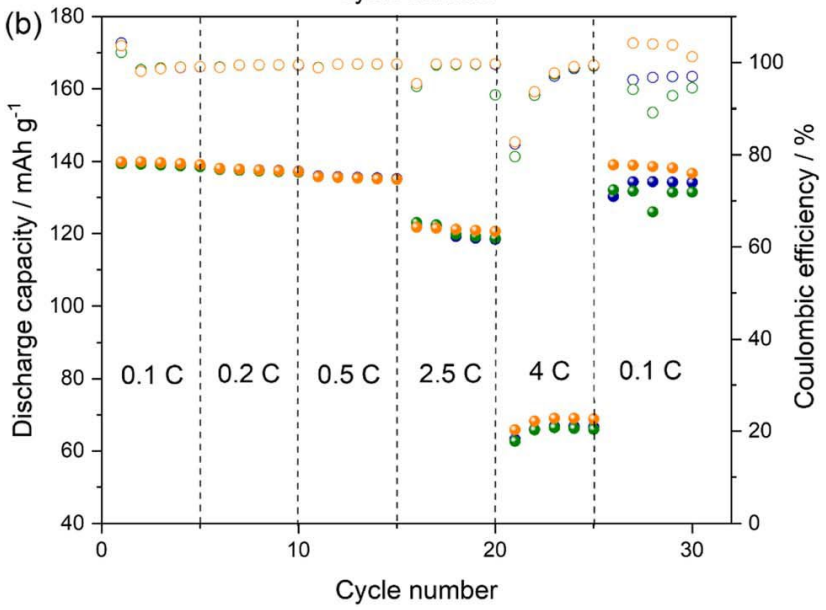

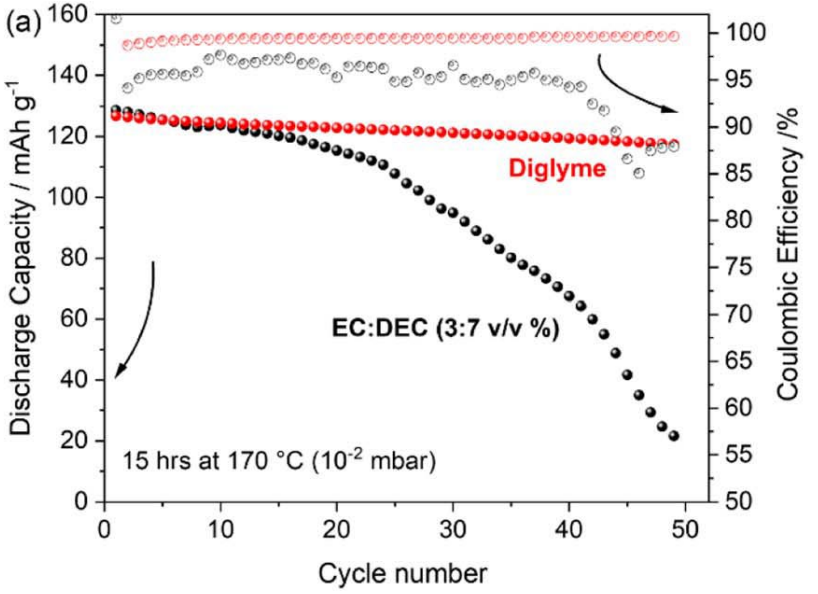

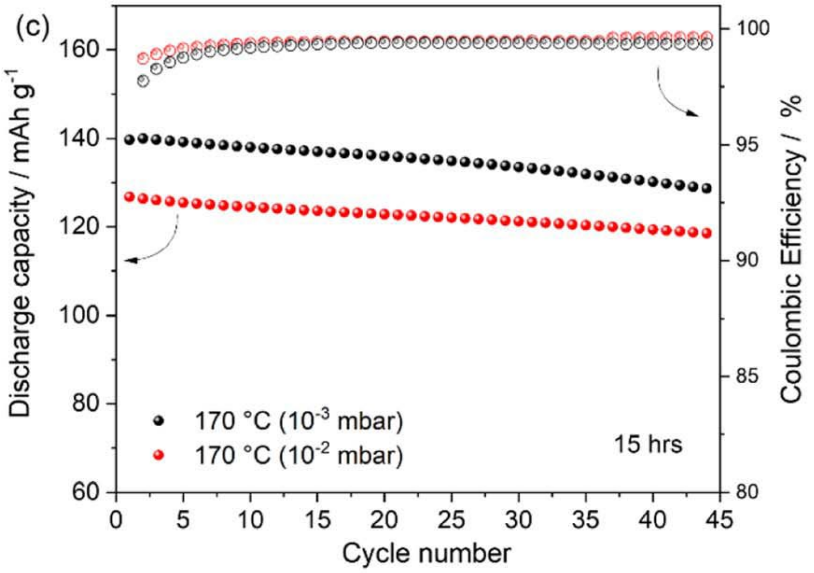

Preheating effect on the phase transitions in PW during cycling

with a current rate of 0.05C, 0.1C, 0.25C in a range between 2 and 4.2 V versus sodium

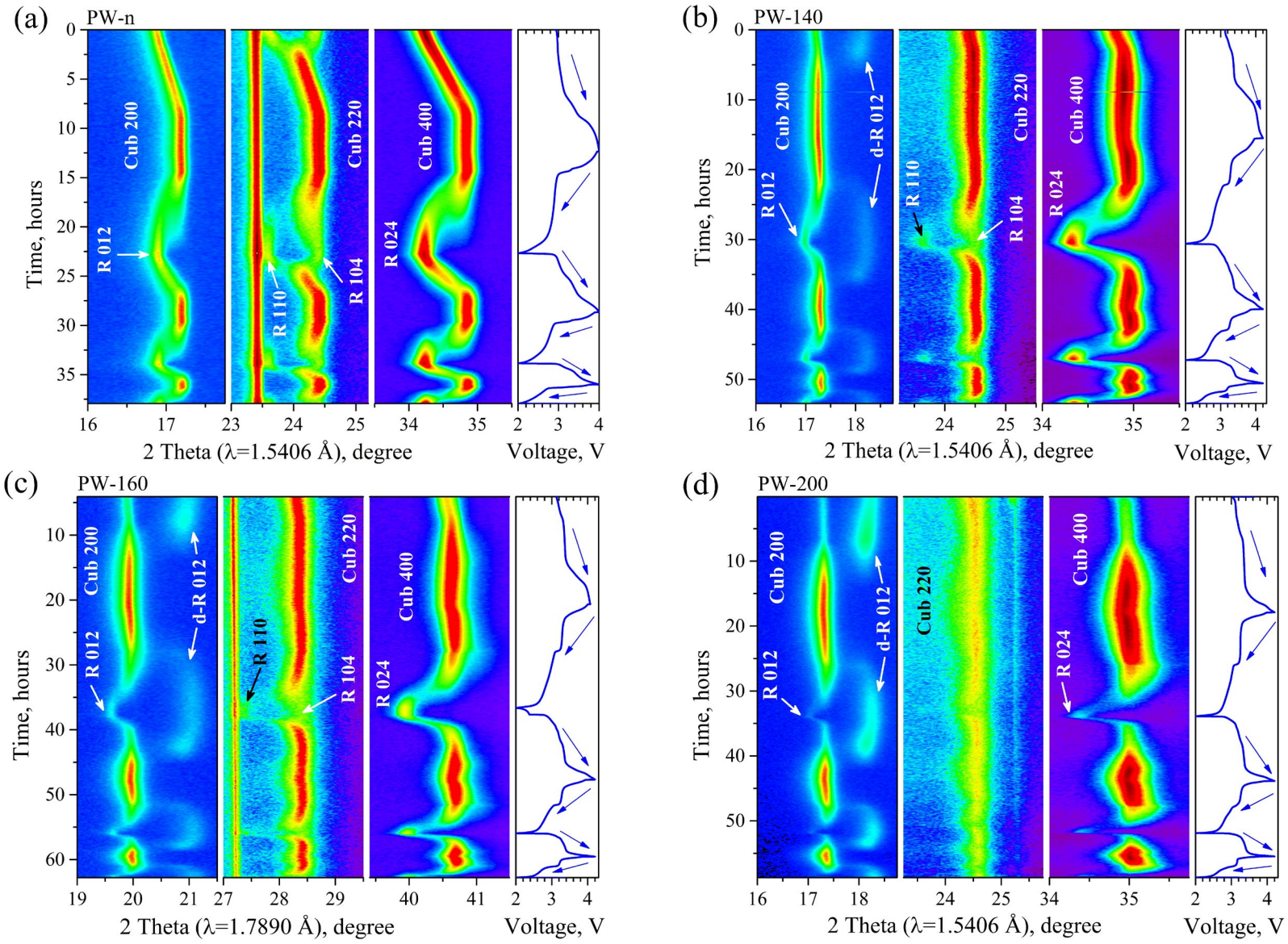

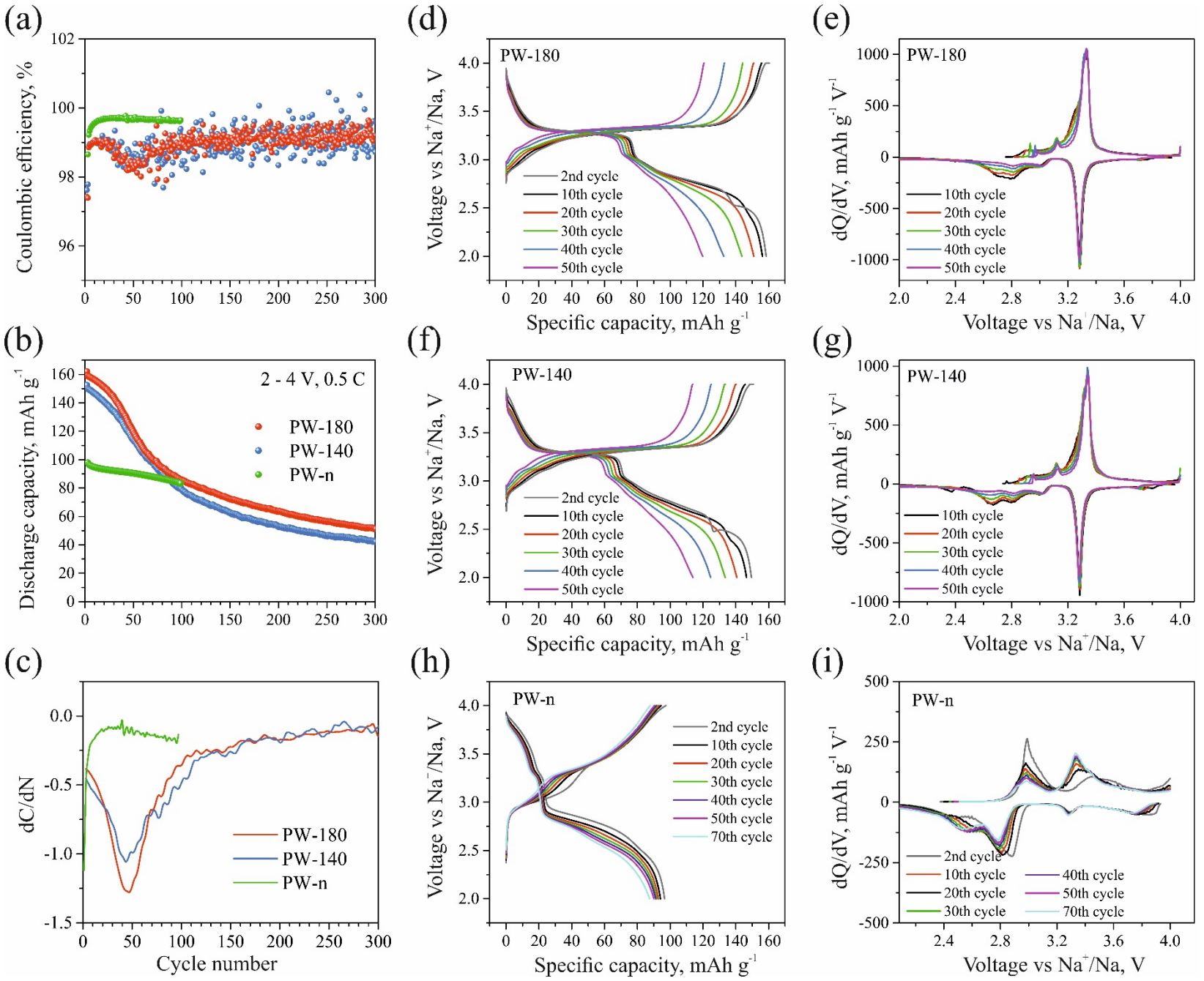
(a)
Coulombic efficiency, %
(b)
Discharge capacity, mAh g-1
2 - 4 V, 0.5 C
PW-180
PW-140
PW-n
(c)
dC/dN
Cycle number
PW-180
PW-140
PW-n
(d)
PW-180
Voltage vs Na+/Na, V
Specific capacity, mAh g-1
2nd cycle
10th cycle
20th cycle
30th cycle
40th cycle
50th cycle
(e)
PW-180
dQ/dV, mAh g-1 V-1
Voltage vs Na+/Na, V
10th cycle
20th cycle
30th cycle
40th cycle
50th cycle
(f)
PW-140
Voltage vs Na+/Na, V
Specific capacity, mAh g-1
2nd cycle
10th cycle
20th cycle
30th cycle
40th cycle
50th cycle
(g)
PW-140
dQ/dV, mAh g-1 V-1
Voltage vs Na+/Na, V
10th cycle
20th cycle
30th cycle
40th cycle
50th cycle
(h)
PW-n
Voltage vs Na+/Na, V
Specific capacity, mAh g-1
2nd cycle
10th cycle
20th cycle
30th cycle
40th cycle
50th cycle
70th cycle
(i)
PW-n
dQ/dV, mAh g-1 V-1
Voltage vs Na+/Na, V
2nd cycle
10th cycle
20th cycle
30th cycle
40th cycle
50th cycle
70th cycle

Structural degradation of the electrodes

PW, 140°C

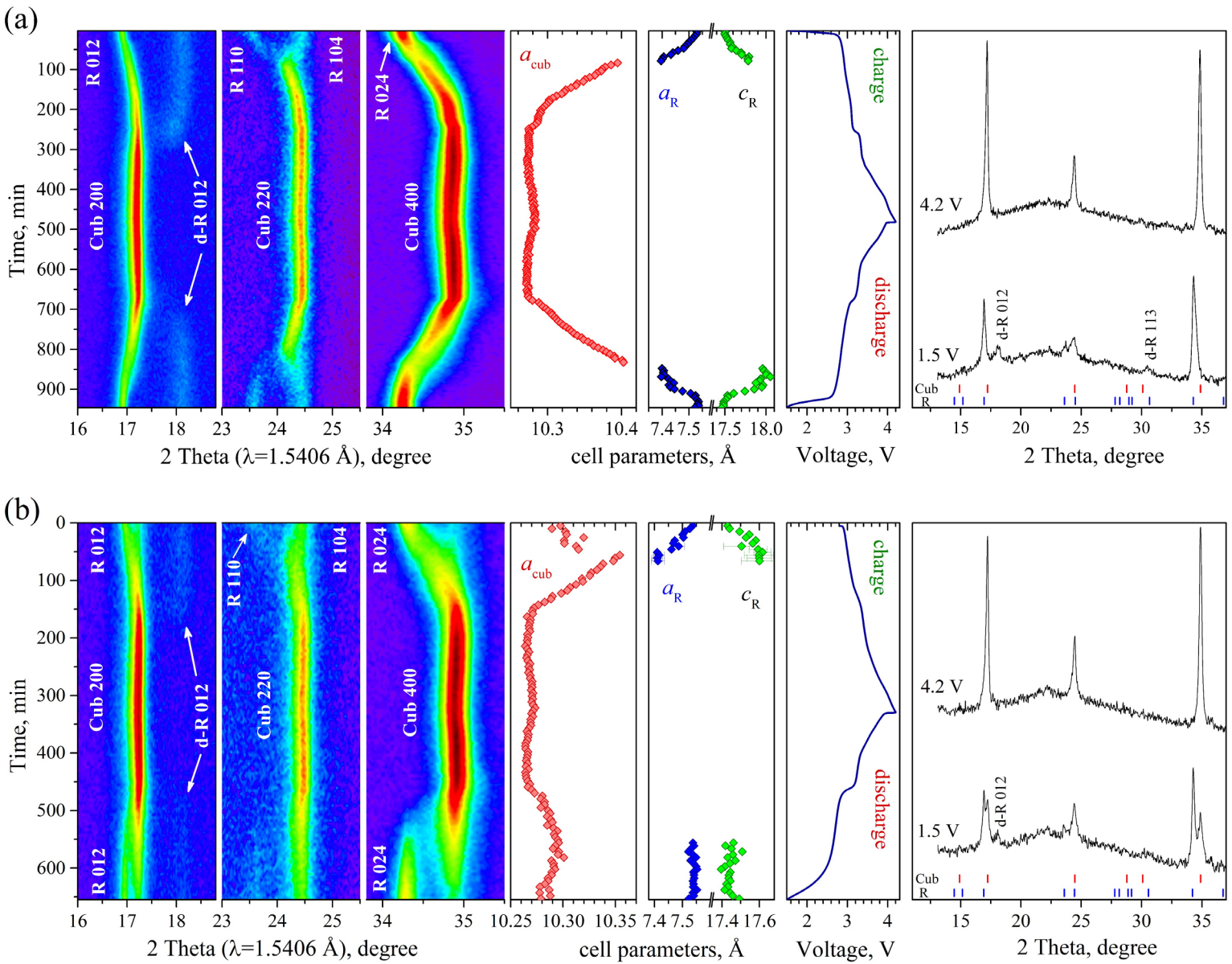

2nd cycle
rate 0.1C

after 350 cycles
rate 0.1C

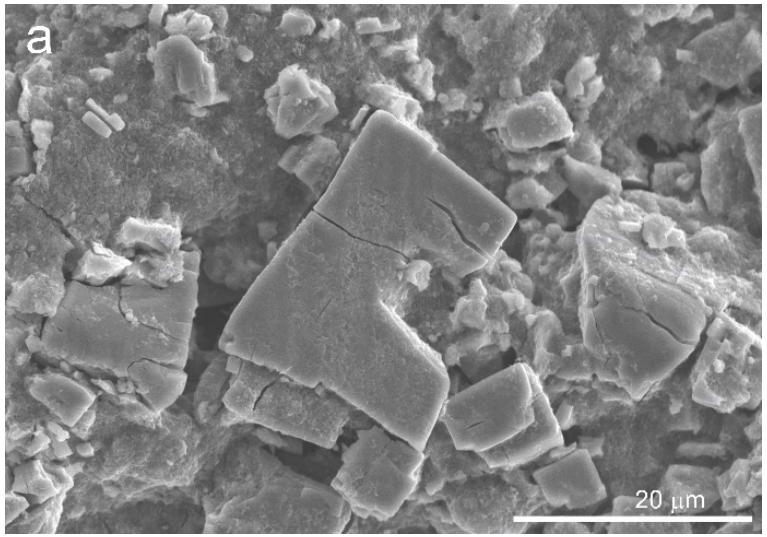

PW_140, initial state

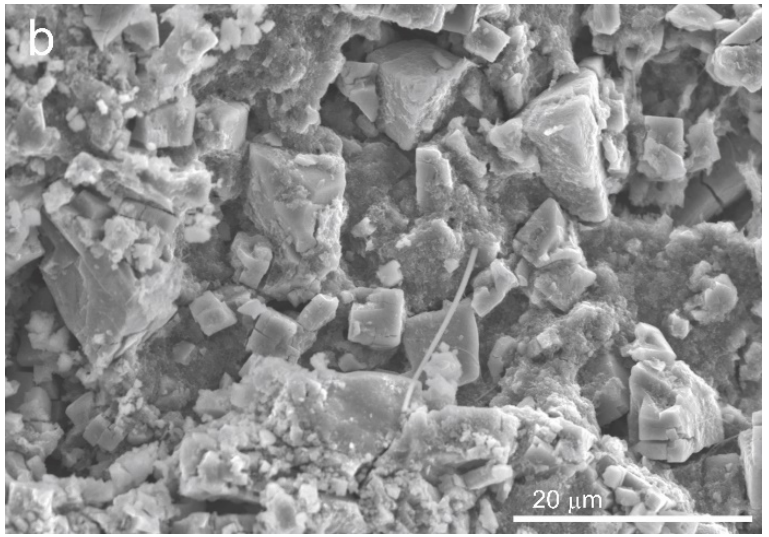

PW_140, after 350 cycles

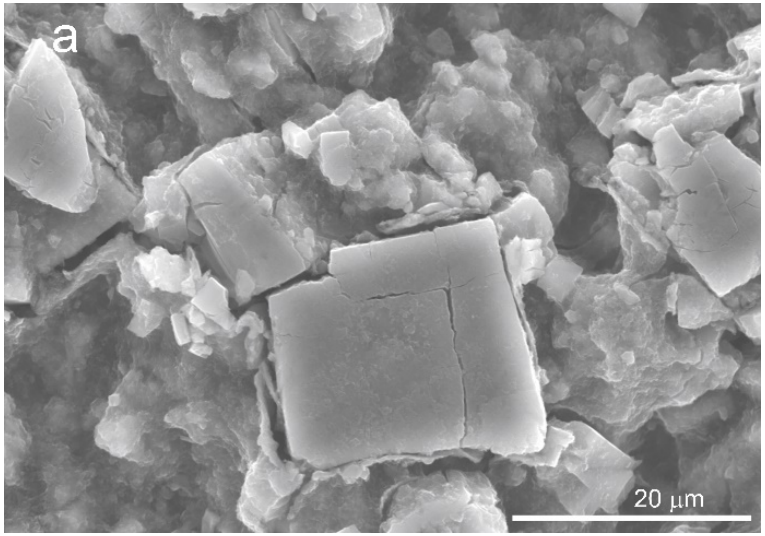

PW_180, initial state

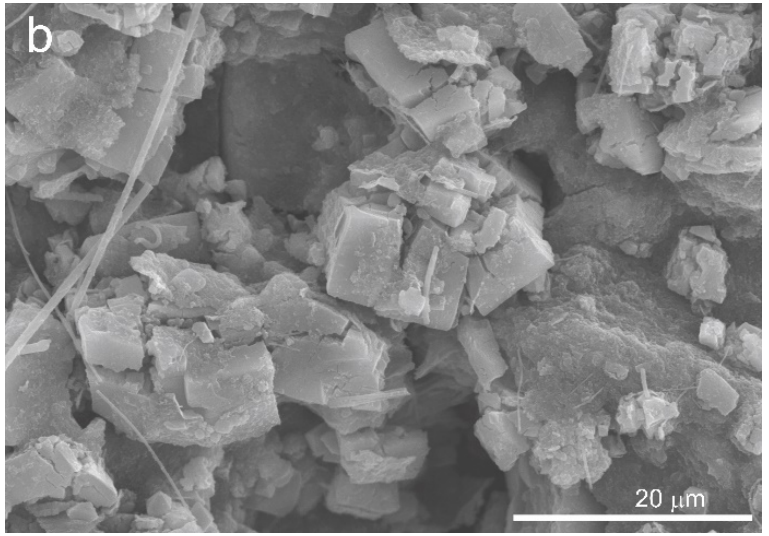

PW_180, after 350 cycles

N.Yu. Samoylova et al., Peculiarities of charge-discharge processes in Prussian white electrodes with different level of dehydration, J. Alloys Compd. 983 (2024) 173849.

Ball milling effect on the structure and electrochemical properties of PW

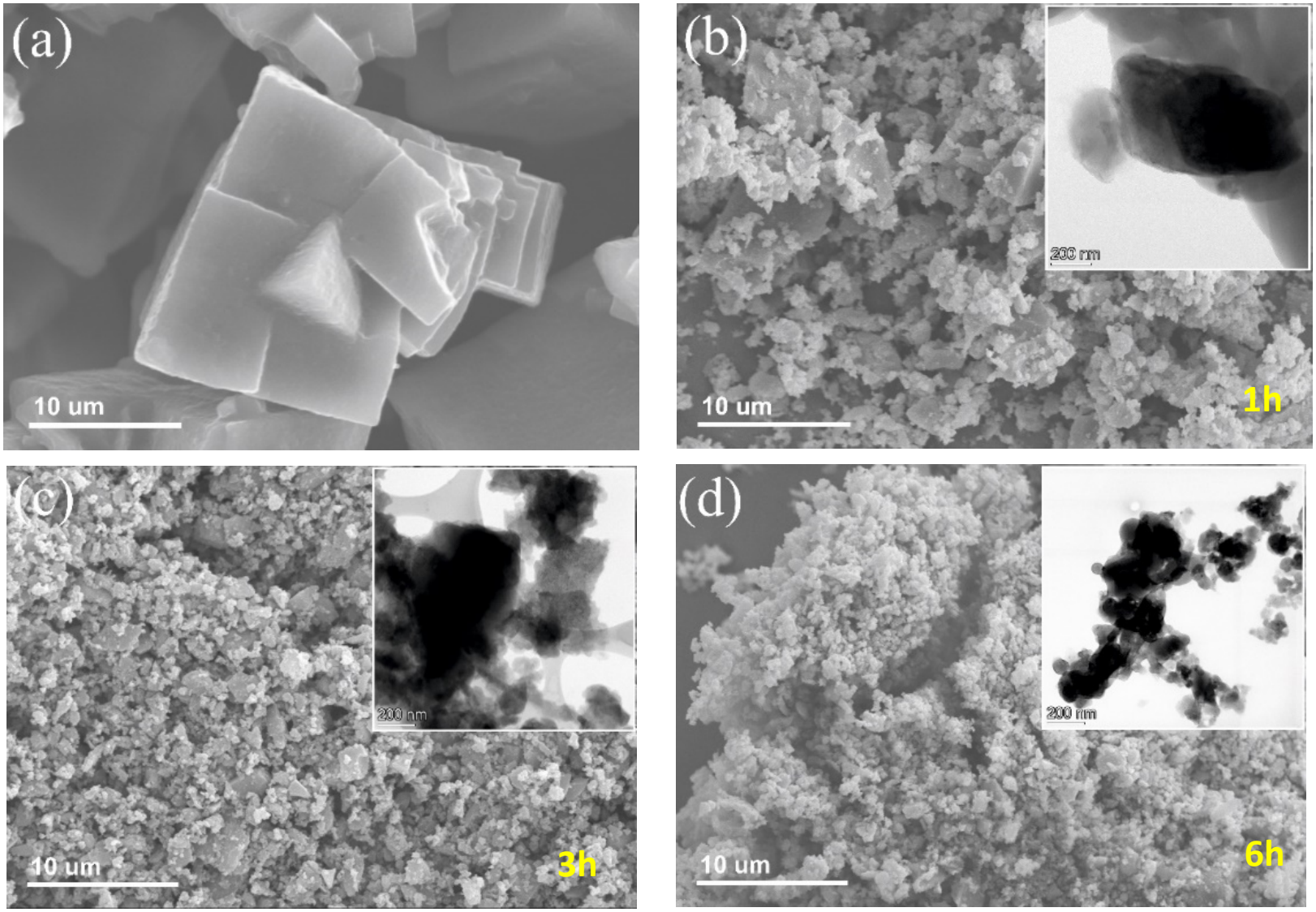

Pristine PW powder was milled (600 rpm) using a planetary ball mill during 1h, 3h and 6h

Phase transitions in the milled PW material during heating

pristine powder

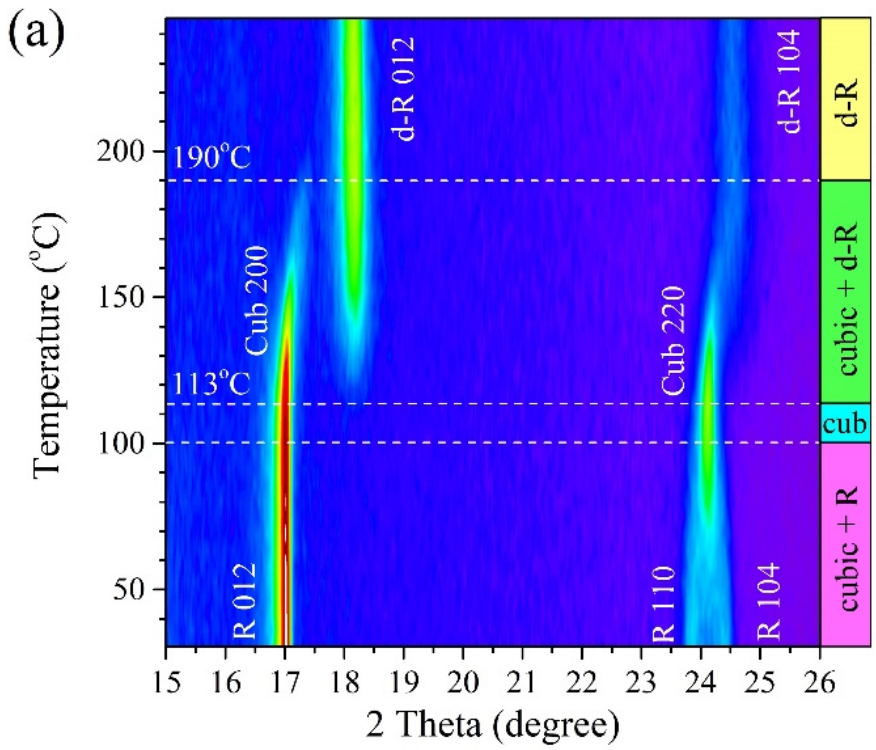

6-h milled powder

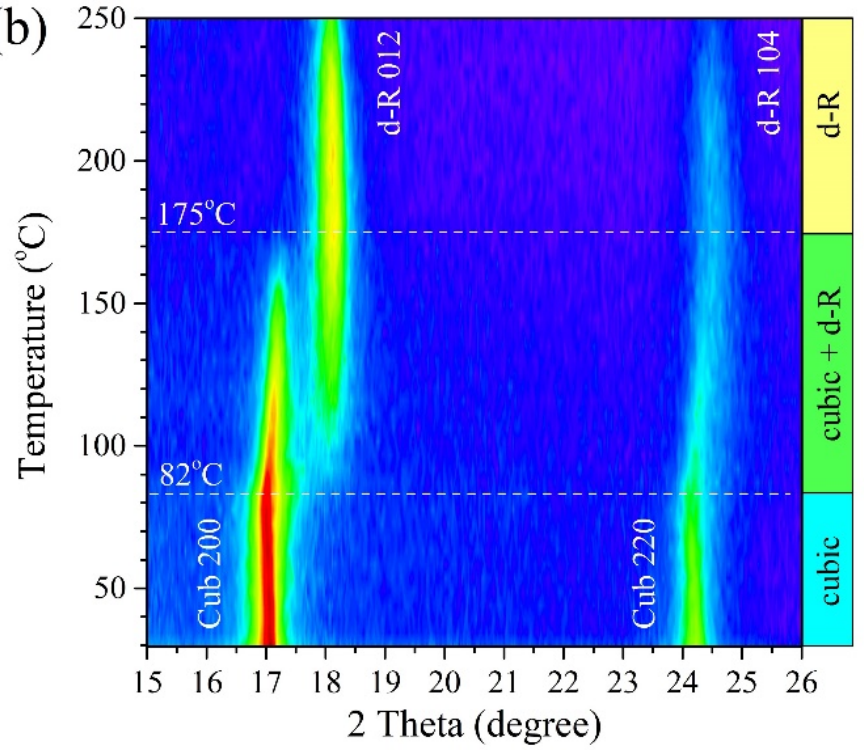

Ball milling decreases the temperature of phase transitions during heating

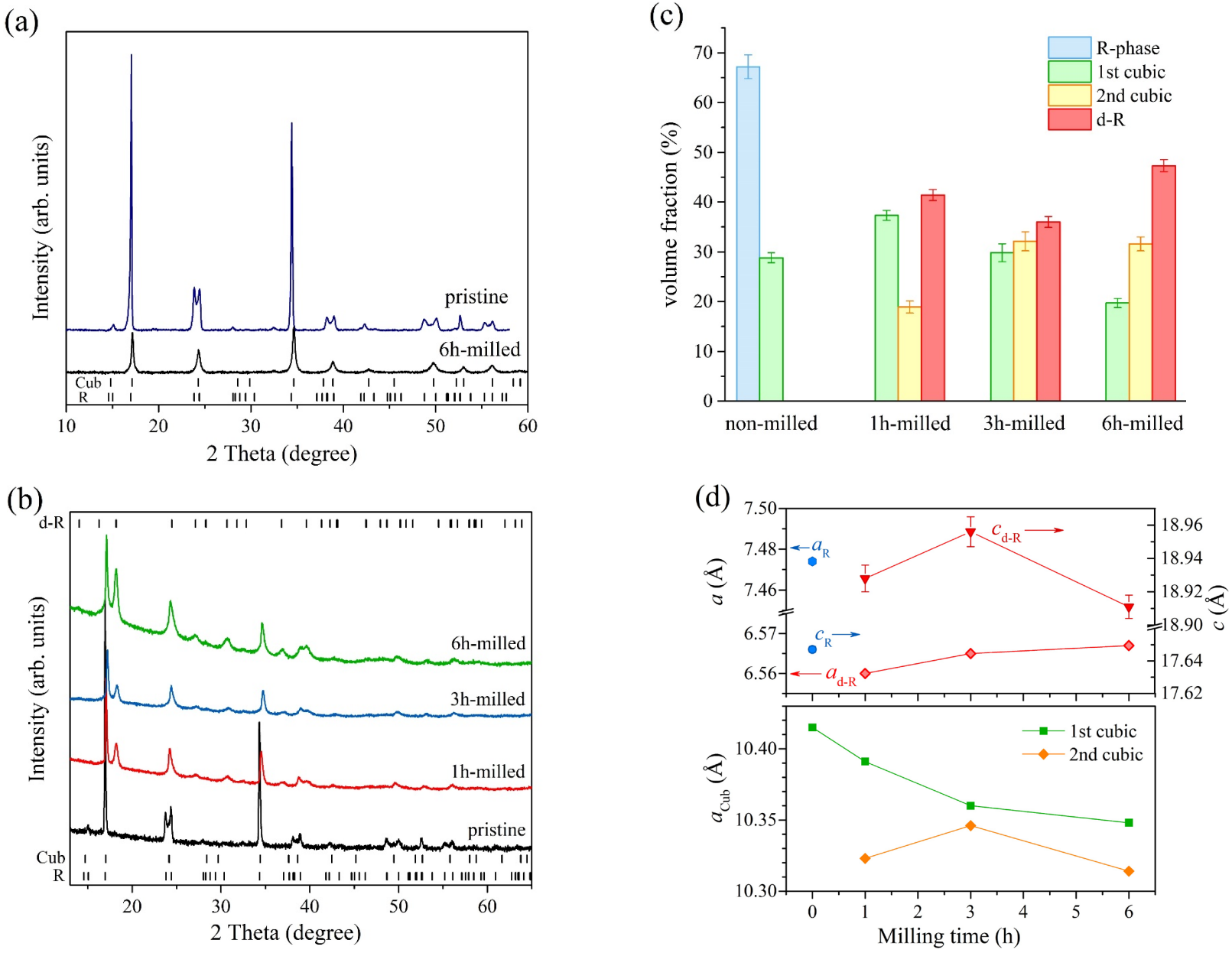
(a)
Intensity (arb. units)
pristine
6h-milled
Cub
R
10
20
30
40
50
60
2 Theta (degree)
(b)
d-R
6h-milled
3h-milled
1h-milled
pristine
Cub
R
Intensity (arb. units)
20
30
40
50
60
2 Theta (degree)
(c)
R-phase
1st cubic
2nd cubic
d-R
volume fraction (%)
0
10
20
30
40
50
60
70
non-milled
1h-milled
3h-milled
6h-milled
(d)
a_R
$c_{d\text{-}R}$
c_R
$a_{d\text{-}R}$
a (Å)
c (Å)
7.50
7.48
7.46
6.57
6.56
18.96
18.94
18.92
18.90
17.64
17.62
1st cubic
2nd cubic
a_{Cub} (Å)
10.40
10.35
10.30
0
1
2
3
4
5
6
Milling time (h)

Phase transitions in the milled PW material during cycling

electrode based on pristine powder

electrode based on 6-h milled powder

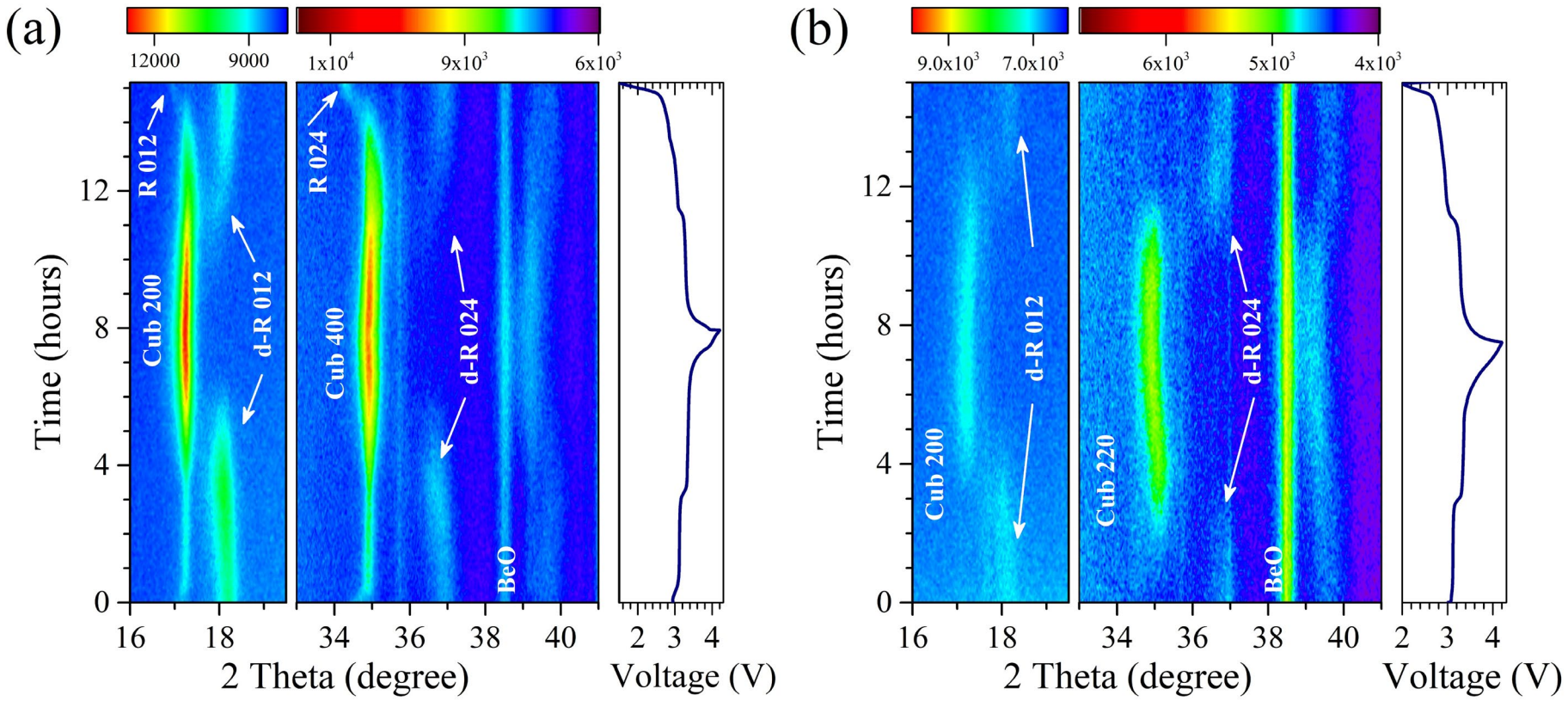

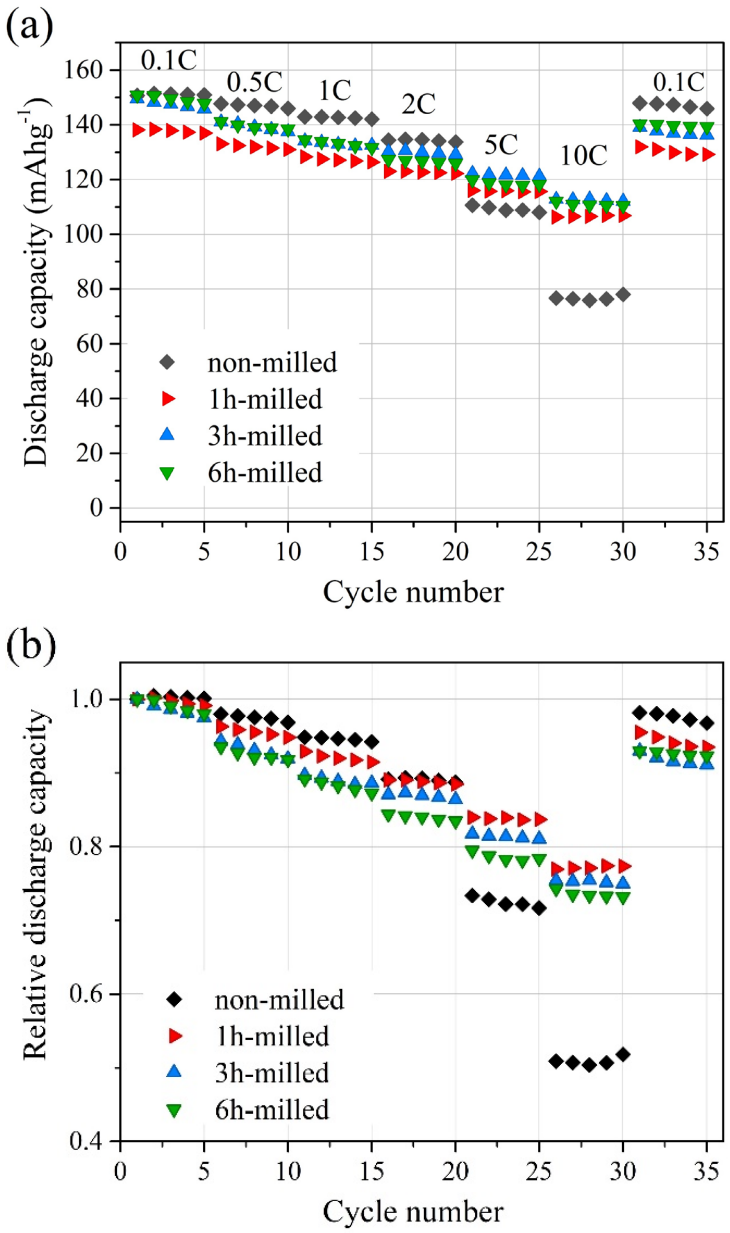
(a)
0.1C
0.5C
1C
2C
5C
10C
0.1C
Discharge capacity (mAhg-1)
Cycle number
non-milled
1h-milled
3h-milled
6h-milled
(b)
Relative discharge capacity
Cycle number
non-milled
1h-milled
3h-milled
6h-milled

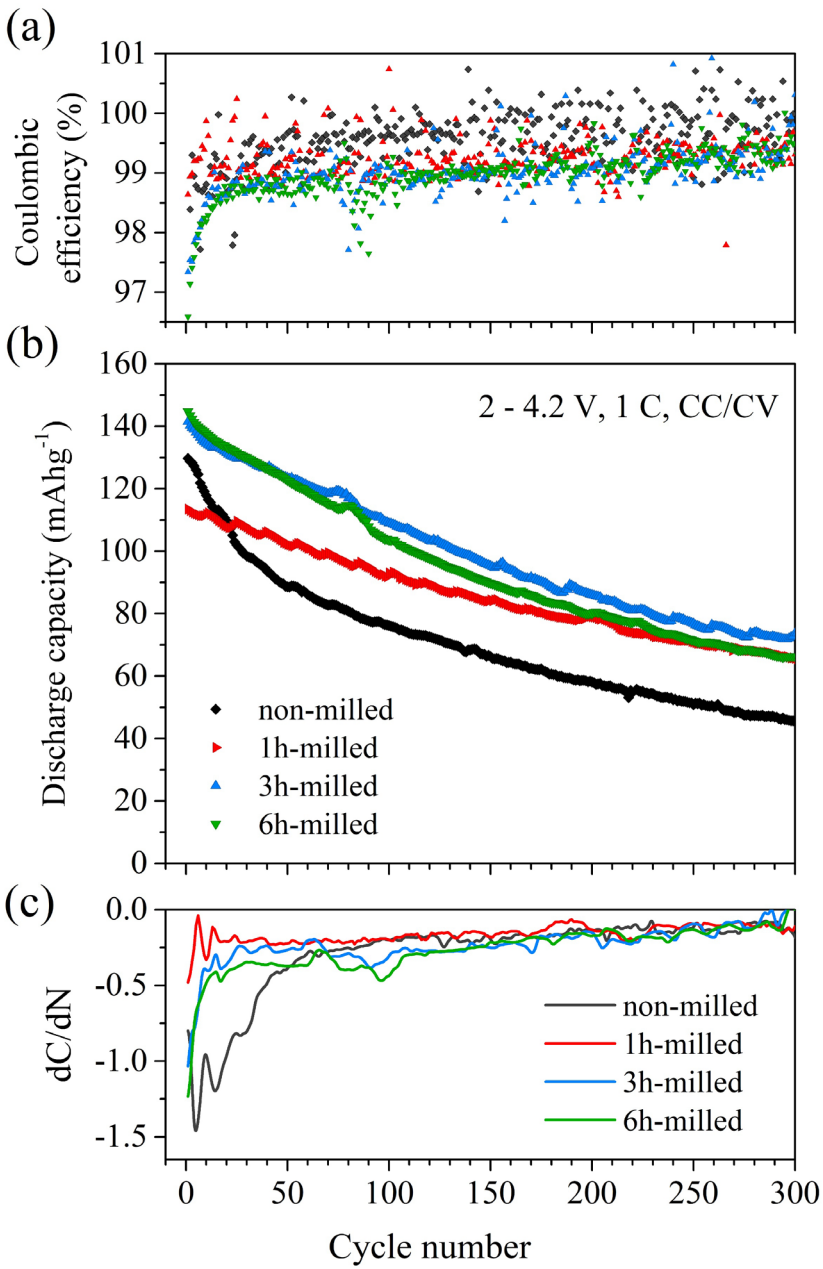
(a)
Coulombic efficiency (%)
(b)
2 - 4.2 V, 1 C, CC/CV
Discharge capacity (mAhg-1)
non-milled
1h-milled
3h-milled
6h-milled
(c)
dC/dN
non-milled
1h-milled
3h-milled
6h-milled
Cycle number

Conclusions

Preheating of the electrode at temperatures from 140 up to 200°C promotes formation of a larger fraction of the dehydrated rhombohedral phase, which is proportional to the temperature of preheating, and results in higher capacity.

The heating process not only removes water from the structure, but also decomposes the PW material at temperature above 180°C.

Operando XRD experiments demonstrate that the PW material degradation during continuous electrochemical cycling occurs in both electrodes, preheated at 140°C and 180°C.

The amount of carbon additive has a more pronounced impact on the capacity of the PW electrodes than a variation of preheating temperature. The electrode with 15 wt.% of carbon has specific capacity values of 160 mAh g^{-1} and 83 mAh g^{-1} at 0.1 C and 10 C cycling rates, exceeding the capacity values previously reported for the same PW material.

Particle fragmentation due to milling leads to more effective dehydration during heating, shifts the phase transition from the cubic phase into the dehydrated rhombohedral phase during heating to lower temperatures, and decreases a number of phase transformations in the material during electrochemical performance. Compared to the pristine PW, the milled material shows a much higher capacity at high cycling rates (110 mAh g^{-1} at 10C) and a smaller capacity drop after long-term cycling.

Summing up, the development of conductive and protective coatings for PW particles and the design of particles (form, size) seem to be more perspective for further investigations aimed at improving the characteristics of PW-based rechargeable batteries.

Thank you for your attention!